Desalination and Water Treatment
www.deswater.com
doi: 10.1080/19443994.2013.769665

51 (2013) 6115–6129
September

Taylor & Francis
Taylor & Francis Group

Sorption behavior of freshwater aquatic fern *Azolla filiculoides* on redwine dye

Pugalendi Suganthi Rani, Rajasekaran Lakshmi Priya, Manickam Velan*

Department of Chemical Engineering, A.C. College of Technology, Anna University, Sardar Patel Road, Chennai 600 025, India
Tel. +91 44 22359117; Fax: +91 44 22355373; email: velan@annauniv.edu

Received 26 November 2011; Accepted 14 January 2013

ABSTRACT

The biosorption of redwine dye from aqueous solution onto aquatic fern *Azolla filiculoides* has been studied. The factors affecting the sorption process, such as solution pH, contact time and initial concentration, adsorbent size, and dosage were determined in the batch mode. Equilibrium sorption isotherms and kinetics were investigated. Sorption isotherm data were fitted with Langmuir and Freundlich models and Langmuir monolayer coverage was determined as 86.21 mg/g. The kinetic data obtained at different initial concentrations were analyzed using pseudo-first-order and pseudo-second-order equations. Biosorption mechanism using Boyd's plot confirmed the film diffusion was the rate-limiting step. The morphological characteristics and functional groups responsible for the binding of dyes were done using Scanning Electron Microscopy and Fourier Transform Infrared Spectroscopy analysis, respectively. The ability of *A. filiculoides* to remove redwine dye from aqueous solution was also examined in an up-flow packed column (continuous mode) at different experimental conditions. The maximum uptake (5.4 mg/g) was obtained at bed height of 15 cm, flow rate of 2 mL/min, and initial dye concentration of 70 mg/L. The Bed Depth Service Time, Thomas, and Yoon and Nelson models were used to analyze the experimental data and the model parameters were evaluated. Thus, *A. filiculoides* has a potential to be a biosorbent for the removal of reactive redwine dye from aqueous solutions.

Keywords: *Azolla filiculoides*; Aquatic fern; Redwine dye; Adsorption isotherms; Biosorption mechanism; Kinetics

1. Introduction

The world's ever increasing population and its progressive adaptation to industry-based lifestyle have inevitably led to an increased anthropogenic impact on the biosphere [1]. In that, textile dyeing is a major industry to consume a large quantity of water and producing large volume of wastewater. Textile wastewater is a complex and highly variable mixture of many polluting substances, including dye which includes persistent color coupled with organic load leading to the disruption of the total ecological balance of the receiving water stream [2].

The variable nature of effluents makes the treatment process complex in nature and needs special attention towards the combination of processes for efficient dye removal. A number of processes like

*Corresponding author.

chemical coagulation, flocculation, precipitation, ozonation, and adsorption have been employed for the treatment of dyes containing wastewaters. The above processes possess inherent limitations such as formation of hazardous by-products, high cost, and higher energy requirements. To overcome these demerits, a number of biological processes such as biosorption, bioaccumulation, and biodegradation have been proposed as having potential application in removal of dyes. Furthermore, biosorption methods often provide better results than activated carbon and natural zeolites and are comparable to synthetic ion-exchange resins [3]. The main attractions of biosorption are high selectivity and efficiency, cost effectiveness, and good removal performance. The use of waste material in biosorption is most advantageous; in fact, the dead organisms, tree leaves, ferns, and seeds are not affected by toxic wastes, do not require a continuous supply of nutrients, and are reused for many cycles and extended periods at room temperature without putrefaction. Many investigators have studied the feasibility of using low cost materials, such as waste banana pith [4], walnut shells [5], eucalyptus bark [6], mango seed husks [7], *Luffa cylindrica* [8], and *Aspergillus niger* [9] as adsorbents for the removal of various dyes from effluents. Materials such as *Spirogyra rhizopus* [10], *Corynebacterium glutamium* [11], Hazelnut shell ash [12], and *Sargassum muticum* [13] have shown extraordinary uptake capacities.

Aquatic ferns have been found to be potential biosorbents because of their fast and easy growth, their wide availability, and their special surface property that enable them to adsorb different kinds of metallic and organic pollutants from solutions. Their cell wall offers a host of functional groups including amino, carboxyl, sulfate, phosphate, and imidazoles associated with polysaccharides, alginic acid, and proteins for binding various pollutants [14]. The aquatic fern *Azolla filiculoides* has been used as adsorbent for acidic and basic dyes by Padmesh et al. [15] and Chiyun Tan et al. [16], respectively. No work has been carried out on biosorption behavior of *A. filiculoides* on reactive dyes. Hence, in this study, we have investigated the biosorption potential of *A. filiculoides* on reactive redwine dye by batch and continuous modes.

2. Materials and methods

2.1. Biosorbent and chemicals

A. filiculoides was collected from the Tamil Nadu Agricultural University, Coimbatore, India. The collected Azolla was shade-dried, crushed, and sieved to particles in the range of 0.25–3.35 mm. Crushed particles were then treated with 0.1 M HCl for 5 h in orbital shaker at a speed of 150 rpm followed by washing with distilled water, and then kept in oven at 60˚C for drying and the dry biomass was used in sorption experiments.

Reactive redwine dye (synthetic dye) was obtained from Chemistor dye manufacturer in powder form and aqueous stock solution (1,000 mg/L) was prepared using distilled water. Then, the desired concentration of experimental solutions was obtained by dilution. The required solution pH was achieved by adding 0.1 M HCl or 0.1 M NaOH solution.

2.2. Batch experiments

About 100 mL of dye solution was taken in a 250 mL Erlenmeyer flask with a biomass of 0.1 g. The biomass and dye solution were allowed to contact well by using a rotary shaker at 150 rpm. At various time intervals, an aliquot of dye solution was centrifuged and the supernatant was used for the determination of dye content using a UV spectrophotometer at 555 nm. The amount of dye biosorbed was calculated by the following equation

$$q_e = \left(\frac{(C_0 - C_e)\,V}{M}\right) \tag{1}$$

where q_e is the equilibrium dye uptake (mg/g), C_0 and C_e are the initial and equilibrium concentration of dye solution (mg/L), V is the volume of the dye solution (L), and M is the Mass of biosorbent added (g).

Similarly, series of experiments were carried out to optimize the process conditions such as pH, contact time, concentration, particle size, and dosage by varying the particular parameter and keeping other parameters constant.

The equilibrium data were analyzed using Langmuir [17] and Freundlich [18] isotherms.

$$\text{Langmuir isotherm: } q_e = \frac{q_{max} K_L C_e}{1 + K_L C_e} \tag{2}$$

$$\text{Freundlich isotherm: } q_e = K_F C_e^{\frac{1}{n}} \tag{3}$$

where q_{max} is the maximum dye uptake (mg dye/g biomass) and K_L is the Langmuir equilibrium constant (L/mg); K_F is the Freundlich constant (L/g) and n is the Freundlich exponent.

The kinetics of the dye uptake was described with pseudo-first-order [19] and pseudo-second-order [20,21] models. The linearized forms of pseudo-first- and pseudo-second-order models are shown below:

$$\log(q_e - q_t) = \log(q_e) - \frac{K_1}{2.303}t \quad (4)$$

$$\frac{t}{q_t} = \frac{1}{K_2 q_e^2} + \frac{1}{q_e}t \quad (5)$$

where q_t is the amount of dye sorbed at time t (mg/g), q_e the equilibrium dye uptake (mg/g), K_1 the first-order rate constant (1/min), and K_2 is the second-order rate constant (g/mg/min).

Scanning Electron Microscopy (SEM) and Fourier Transform Infrared Spectroscopy (FTIR) analysis had been carried out to determine the morphological changes before and after sorption of dyes, and the functional groups responsible for the sorption of dyes onto Azolla, respectively. Chemical Oxygen Demand (COD) analysis was also performed for dye solution kept at optimum process conditions by open reflux method [22].

2.3. Column studies

Continuous-flow sorption experiments were conducted in a glass column of internal diameter 1.5 cm and length of 35 cm. Since the ratio of column diameter to particle diameter is high, the effect of channeling has negligible effect [15]. The column was loaded with 3.1, 5.3, and 7.6 g of biomass to yield 5, 10, and 15 cm bed heights, respectively. The dye solution at a concentration of 35 and 75 mg/L was pumped through the column using peristaltic pump at a flow rate of 2, 4, and 6 mL/min. At regular time intervals, the dye solution was collected at the outlet of the column and analyzed for its concentration.

The breakthrough time (t_b, the time at which dye concentration in the effluent reached 5% of the inlet concentration) and the bed exhaustion time (t_e, the time at which dye concentration in the effluent equals inlet concentration) were used to evaluate the breakthrough curves. The mass of dye adsorbed (m_{ad}) in the column was calculated from the area above the breakthrough curve (concentration vs. time) multiplied by the flow rate [23]. Dividing the dye mass adsorbed (m_{ad}) by the sorbent mass (M) leads to uptake capacity (q_e) of the biomass.

The breakthrough time and the bed exhaustion time were used to evaluate the mass transfer zone (Δt) given by equation as follows [23],

$$\Delta t = t_e - t_b \quad (6)$$

Total amount of dye sent to the column (m_{total}) can be calculated as follows [24],

$$m_{total} = \left(\frac{C_0 Q\, t_e}{1,000}\right) \quad (7)$$

Total dye removal (%) with respect to flow volume can be calculated from the ratio of dye mass adsorbed (m_{ad}) to the total amount of dye sent to the column (m_{total}) as described [23],

$$\text{Total dye removal}\,(\%) = \left(\frac{m_{ad}}{m_{total}}\right)100 \quad (8)$$

Using the column details, various models like Bed Depth Service Time (BDST) [25], Thomson [26], and Yoon and Nelson [27] were employed.

3. Results and discussion

3.1. Batch experiments

3.1.1. Effect of pH

The pH of the dye solution played an important role in the biosorption of dyes. To study the effect of pH on equilibrium uptake capacity of biomass, experiments were conducted at 50 mg/L initial dye concentration, 120 min of contact time, and 0.10 g biomass dose at 30°C.

The dye uptake was sensitive to pH variations in the examined range of 2–8 (2, 3 … 8) and the amount of dye adsorbed decreased with increase in pH. This indicated that the reactive groups of the dye molecules are cationic while the functional groups (such as carboxyl, phosphate, and sulfonyl group) present on the surface of biosorbent were anionic type [28]. As the pH increased, the cationic charge decreased and hence, biosorption of reactive redwine dye decreased. The maximum uptake of 10.32 mg/g was obtained at pH of 3.0. Similarly, Hu reported that the maximum adsorption of different reactive dyes on the *Aeromonas* sp. biomass was observed at pH 3.0 [29]. Yakup Arica and Gulay Bayramoglu studied biosorption of reactive red 120 dye on *Lentinus Sajor-caju* biomass and the maximum dye biosorption was observed at pH 3.0 [30].

3.1.2. Effect of contact time and initial concentration

The effect of initial concentration (50, 100, and 150 mg/L) on adsorption of the redwine dye onto pretreated *A. filiculoides* was studied at pH 3, 0.1 g/L of biomass dosage, and 30°C. The results are shown in Fig. 1. From the figure, it could be seen that the amount of redwine dye adsorption increased from

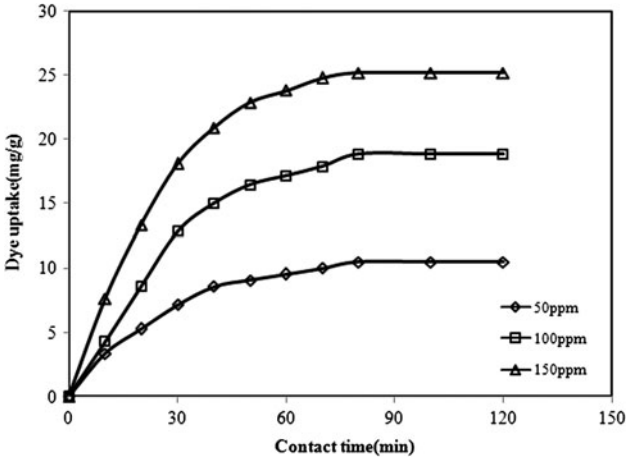

Fig. 1. Effect of contact time and initial concentration on the adsorption of redwine dye by *A. filiculoides* (pH 3, 0.10 g biomass, and 30˚C).

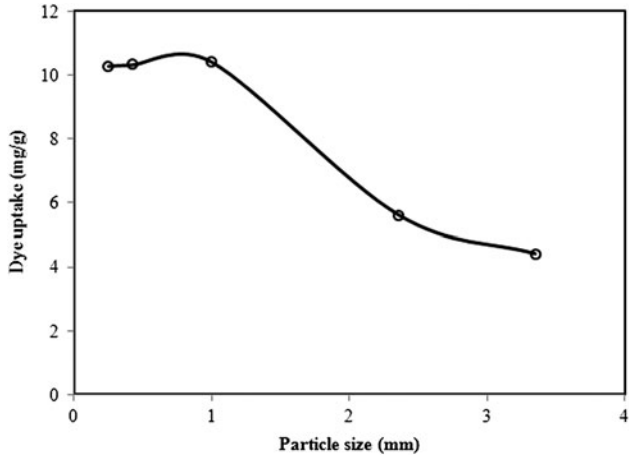

Fig. 2. Effect of particle size on the adsorption of redwine dye by *A. filiculoides* (pH 3, 50 mg/L dye concentration, 0.10 g biomass, and 30˚C).

10.47 to 25.16 mg/g with the increase in initial dye concentration from 50 to 150 mg/L. This suggests that initial concentration provides an important driving force to overcome all mass transfer resistance of the redwine dye between the aqueous and solid phase. Therefore, a higher initial concentration of dye will enhance the adsorption process [31].

Fig. 1 also shows the rapid adsorption of redwine dye during the first 30 min for all initial concentrations, and thereafter, the adsorption rate decreases till it reaches equilibrium. The rapid adsorption was due to the bare surface of sorbent at the initial stage. Hence, the sorption rapidly occurred and usually controlled by the diffusion process from the bulk to the surface. But in later stage, the stabilized sorption was due to less available sites indicating that the biosorbent was saturated at that level [32].

3.1.3. Effect of particle size and biomass dosage

Influence of particle size (Fig. 2) on dye uptake upon *A. filiculoides* was studied (at pH 3, initial concentration of 50 mg/L, and 30˚C) using five different particle sizes from 0.25 to 3.35 mm, and found that dye uptake capacity decreased as the particle size increased from 10.41 to 4.58 mg/g. This might be due to the fact that the smaller particles favor biosorption with very high uptake because of higher surface area per unit weight.

The effect of biosorbent dosage on the removal of redwine dye by the biosorbent *A. filiculoides* was examined at 50 mg/L dye concentration by varying the dosage from 0.1 to 0.6 g of biomass in 100 mL of the dye solution and the results are shown in Fig. 3.

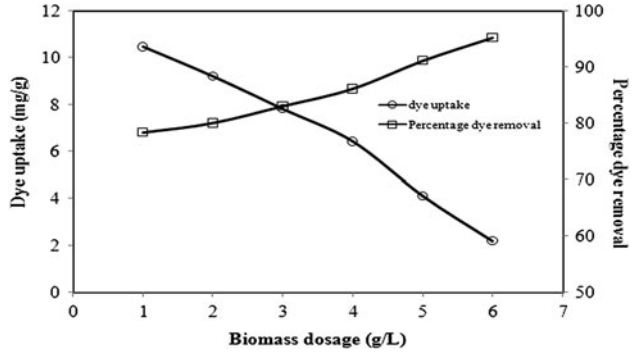

Fig. 3. Effect of biosorbent dosage on the adsorption of redwine dye by *A. filiculoides* (pH 3, 50 mg/L dye concentration at 30˚C).

It could be seen from the figure that removal efficiency (%) increased from 78.35 to 95.21% while the dye uptake per unit weight of adsorbent decreased from 10.45 to 2.2 mg/g. The decrease in dye uptake with increase in dosage might be due to the decrease of surface area of the biosorbent by the overlapping or aggregation during the sorption [33]. Hence, the biomass dosage of 0.1 g/L was chosen for biosorption study.

3.2. Kinetic studies

In order to obtain the first-order rate constants and an equilibrium dye uptake, the straight line plots of ln $(q_e - q_t)$ against t were made. If the plot was found to be linear with good correlation coefficient, it indicates that pseudo-first-order would be appropriate and the adsorption process would be a pseudo-first-order process. The rate constants and equilibrium uptake

determined from the modeling are summarized along with corresponding correlation coefficients in Table 1. It could be seen from the table that the values of the correlation coefficients of the pseudo-first-order model were higher than those of the second-order model; further, the estimated q_e values of first-order model were much more accurate than the second-order model. The accurate prediction of q_e values and goodness-of-fit indicated that the pseudo-first-order model better described the adsorption of redwine dye on *A. filiculoides*. Similar results are obtained by Vilar et al. for algal biomass based materials [34].

The pseudo-second-order model is based on the sorption capacity on the solid phase. Contrary to other well-established models, it predicts behavior over the whole range of studies and it is in agreement with chemisorptions mechanism. In order to obtain the second-order rate constants and equilibrium dye uptake, the straight line plots of t/q_t against t were made for *A. filiculoides* at various initial dye concentrations. The rate constants, equilibrium uptake, and the corresponding correlation coefficients are summarized in table 1. It could be seen from the table that there was no agreement between q_e experimental and q_e calculated values for the pseudo-second-order model.

3.3. Biosorption mechanism

To find the rate-limiting step is an important factor to be considered in adsorption process [35]. The overall rate of adsorption is controlled by the slowest step, which would be either film diffusion or pore diffusion. From the slope of the plot of square root of time ($t^{0.5}$) vs. dye uptake (mg/g), the intraparticle diffusion coefficient for the adsorption of redwine dye has been calculated (Fig. 4(a)). It was observed that the biosorption process comprised of two phases, suggesting that the intraparticle diffusion was not the rate limiting step for the whole reaction [36]. A first linear portion ended with a smooth curve followed by a second linear portion. The double nature of the curve reflected two-stage external mass transfer followed by intraparticle diffusion. The initial curved portion of the plot indicated boundary layer effect while the second linear portion was due to intraparticle or pore diffusion. The slope of the second linear portion of the plot has been defined as the intraparticle diffusion parameter k_i (mg/g min). The calculated k_i values at various initial dye concentrations are shown in Table 2. The presence of both film and pore diffusion was confirmed by the biphasic nature of intraparticle diffusion plot.

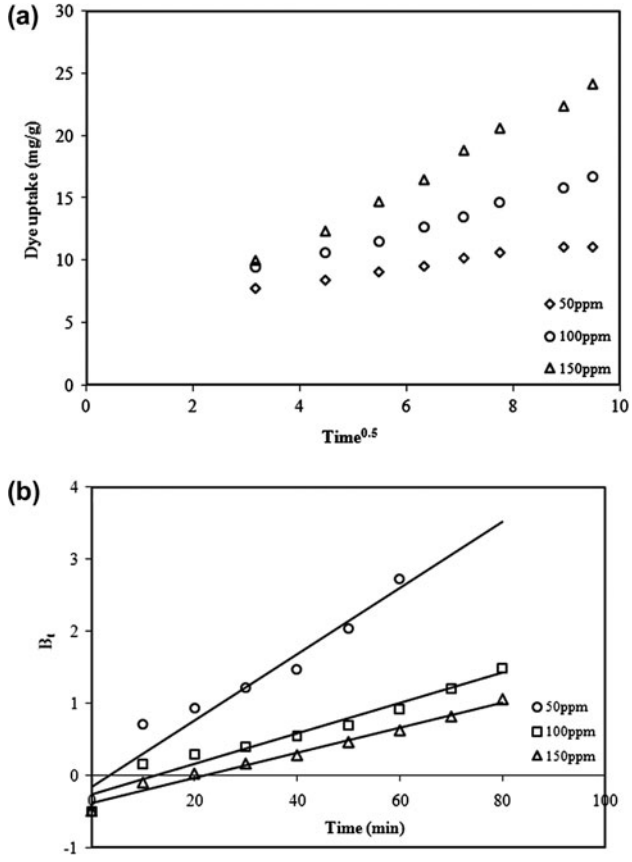

Fig. 4. Biosorption mechanism of redwine dye uptake by *A. filiculoides* (a) Intraparticle diffusion model (b) Boyd plot.

Table 1
Pseudo-first-order and second-order kinetic parameters for the dye sorption onto *A. filiculoides* at various dye concentrations

C_0 (mg/L)	q_e (exp) (mg/g)	Pseudo-first-order			Pseudo-second-order		
		K_1 (l/min)	q_e (cal) (mg/g)	R^2	K_2 (g/mg/min)	q_e (cal) (mg/g)	R^2
50	10.48	0.0967	11.24	0.994	2.09×10^{-3}	14.70	0.992
100	19.28	0.0875	19.68	0.999	4.775×10^{-4}	34.48	0.951
150	26.67	0.0737	27.66	0.993	9.471×10^{-4}	37.03	0.976

In order to predict the actual rate limiting step, the data were further analyzed using Boyd kinetic expression [37],

$$F = 1 - \frac{6}{\pi^2}\exp(-B_t) \tag{9}$$

$$\text{and} \quad F = \frac{q_t}{q_e} \tag{10}$$

where q_e is the amount of dye adsorbed at infinite time (mg/g), q_t the amount of dye sorbed at any time t (mg/g), F the fraction of dye mass adsorbed, and B_t is the mathematical function of F.

To compute B_t, Eq. (9) could be expressed as

$$B_t = -0.4977 - \ln(1 - F) \tag{11}$$

Thus, the value of B_t could be computed for each value of F, and then plotted against time (Fig. 4(b)) to configure the so-called Boyd plots. The linearity of these plots was employed to distinguish between external-transport- (film diffusion) and intraparticle-transport-controlled rates of sorption. A straight line passing through the origin indicated that the sorption processes were governed by particle diffusion mechanisms; or else they were governed by film diffusion [38]. In our case, the plots were neither linear nor passed through the origin (Fig. 5(b)). This indicated that film diffusion was the rate-limiting biosorption process for the adsorption of redwine dye onto *A. filiculoides*. The calculated B_t values were used to calculate the effective diffusion coefficient, D_i (cm^2/s) using the relation:

$$B_t = \pi^2 \frac{D_i}{r^2} \tag{12}$$

where r represents the radius of the particle calculated by sieve analysis assuming the particles as spheres [39]. The calculated D_i values at different initial dye concentrations are provided in Table 2.

3.4. Biosorption isotherms

The experimental biosorption isotherms obtained were analyzed using Langmuir and Freundlich isotherm models and the best-fit model was determined on the basis of non-linear regression correlation coefficient (R^2), Root Mean Square Error (RMSE), and Chi test. The equilibrium data reasonably well represented by two isotherm models are shown in Fig. 5.

Langmuir sorption model served to estimate the maximum dye uptake values where these could not be reached in the experiments. A maximum dye uptake of 86.21 mg/g was obtained. The Freundlich isotherm constants of $1/n$ and K_F were 0.807 and 0.4536, respectively. The value of $1/n$ was between 0 and 1, represented that the biosorption of redwine dye on *Azolla filiculoides* was favorable [16]. On comparing the isotherm models, RMSE, and Chi-square tests, it is concluded that the redwine biosorption data obtained in this study better fitted with the Langmuir form as well as Freundlich form (Table 3).

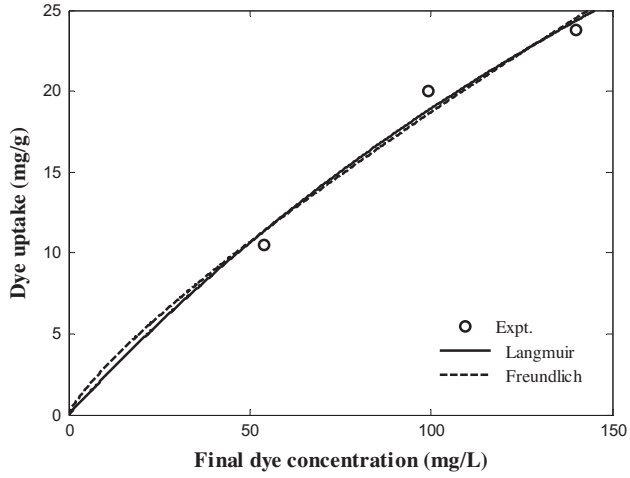

Fig. 5. Application of Langmuir and Freundlich isotherm models to experimental data obtained during adsorption of redwine dye by *A. filiculoides*.

Table 2
Intraparticle diffusion constant and effective diffusivity at various initial dye concentrations

C_0 (mg/L)	K_i (mg/g min)	D_i (cm^2/s)
50	0.5699	3.13×10^{-6}
100	1.3686	1.56×10^{-6}
150	1.6766	9.49×10^{-7}

3.5. Thermodynamic parameters

Based on fundamental thermodynamics concept, the Gibbs free energy change, ΔG^0, is the fundamental criterion of spontaneity. The free energy of the sorption reactions, considering the sorption equilibrium constant, K_a, is given by the following equation:

$$\Delta G^0 = -RT \ln K_a \tag{13}$$

where R is the universal gas constant, 8.314 J/mol/K and T is the absolute temperature (K). The Gibbs free

Table 3
Isotherm constants of various models for redwine dye biosorption onto *A. filiculoides*

Isotherms	Isotherms constants at pH 3 and temperature 30°C
Langmuir	
q_{max}	86.21
K_L	0.00281
R^2	0.989
RMSE	1.1
X^2	2.421
Freundlich	
K_F	0.4536
n	1.239
R^2	0.9857
RMSE	1.274
X^2	3.248

energy change, ΔG^0, can also be represented as follows:

$$\Delta G^0 = \Delta H^0 - T\Delta S^0 \quad (14)$$

A plot of ΔG^0 vs. T was linear. Enthalpy change, ΔH^0, and entropy change, ΔS^0, were determined from the slope and intercept of the plots. The values for the sorption equilibrium constant, K_a, decreased with increasing temperature. The Gibbs free energy change, ΔG^0, for the sorption processes at various temperatures 300, 303, and 308 K were −14.22, −14.54, −15.16 kJ/mol, respectively. The negative values of ΔG^0 confirmed the feasibility of the process and the spontaneous nature of sorption with a high preference of redwine dye on *A. filiculoides*. The positive value of ΔS^0 (0.1182 kJ/mol K) reflected the affinity of the *Azolla* for the dye and suggested some structural changes in dye and *Azolla* [40] and also showed the increase of randomness at the solid/liquid interface during the sorption of dye on *Azolla* [41]. The value of ΔH^0 was positive (21.242 kJ/mol), indicating that the sorption reaction was endothermic and might involve chemisorption since it was in the range of 20.9–418.4 kJ/mol. Similar result was obtained by Cai-yun Tan et al. who studied biosorption of basic orange dye on *A. filiculoides* [16].

3.6. Column studies

3.6.1. Effect of flow rate

Flow rate is one of the important parameters in evaluating the sorbent for continuous treatment of dye effluents on an industrial scale. The influence of flow rate was investigated by keeping the initial dye concentration at 70 mg/L adjusted to pH 3 as constant. At a bed height of 5 cm, flow rates of 2, 4, and 6 mL/min were changed and different breakthrough curves obtained were shown in Fig. 6 and related parameters were tabulated in Table 4. In this study, as the flow rate increased, both the dye uptake and percentage of removal get decreased. The increase in flow rate decreased both breakthrough and exhaustion time and volume, which might be due to insufficient residence time of the solute in the column and the diffusion limitations of the solute into the pores of the sorbent [42].

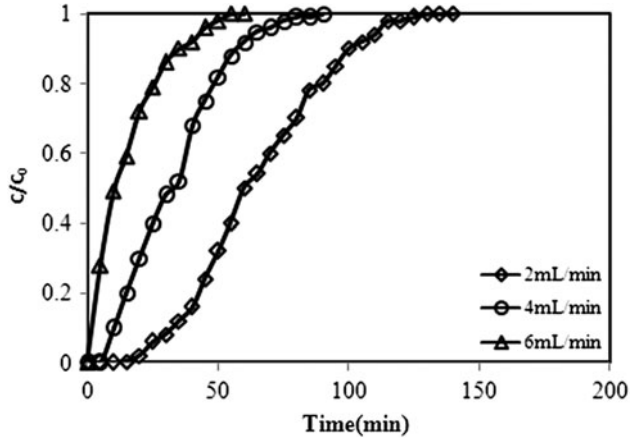

Fig. 6. Breakthrough curves for sorption of redwine dye by *A. filiculoides* at different flow rates (70 mg/L dye solution, 5 cm bed height, and 30°C).

3.6.2. Effect of bed height

In column experiments, breakthrough curves were obtained at different bed heights (5, 10, and 15 cm) and the inlet dye concentration of 70 mg/L and flow rate of 2 mL/min were kept constant. As shown in Fig. 7 and Table 4, breakthrough and exhaustion time as well as volume increased on increasing the bed height, which resulted in a broadened mass transfer zone. The dye uptake at different bed heights were 2.9, 4.09, and 5.4 mg/g, respectively. On contrary, to the flow rate results, high uptake was observed at higher bed height of 15 cm which was due to an increase in the surface area of the biosorbent that provided more binding sites for the sorption [15,43].

3.6.3. Effect of initial dye concentration

The effect of initial dye concentration was determined by keeping the bed height at 15 cm and flow

Table 4
Column data and parameters obtained at different flow rates, bed heights, and initial dye concentrations

Bed height (cm)	Flow rate (mL/min)	Initial dye concentration (mg/L)	Time vs. C/C_0			Throughput volume vs. C/C_0					
			t_b (min)	t_e (min)	$(q_o)_{exp}$ (mg/g)	Bed volume V (mL)	Volume at breakthrough (mL)	Bed volumes at V_b	Volume at exhaustion V_e (mL)	Bed volumes at V_b	$(q_o)_{exp}$ (mg/g)
5	2	70	18	130	2.9	8.83	55	6	230	26	2.09
10	2	70	37.5	390	4.09	17.66	120	7	580	33	3.16
15	2	70	60	570	5.4	26.5	280	11	950	37	4.01
5	4	70	6	85	2.6	8.83	32	4	260	29	2.06
5	6	70	2	55	1.8	8.83	6	1	262	30	1.45
15	2	35	120	560	3.0	8.83	–	–	–	–	–

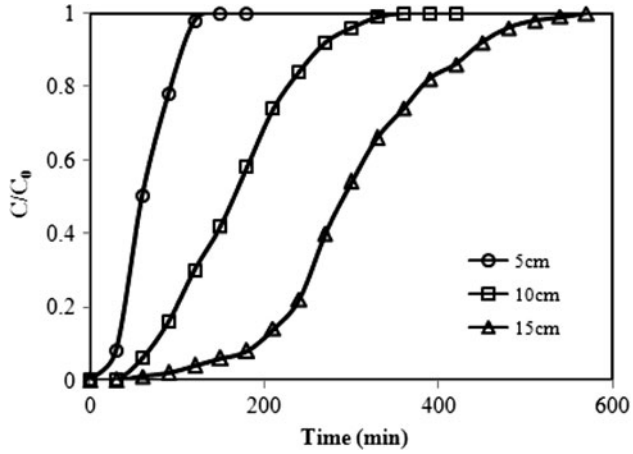

Fig. 7. Breakthrough curves for sorption of redwine dye by *A. filiculoides* at different bed heights. (70 mg/L dye solution, 2 mL/min, and 30 °C).

rate at 2 mL/min as constant. The breakthrough curves obtained for different initial dye concentrations were shown in Fig. 8. Delayed breakthrough curves were seen as the inlet dye concentration increased; the lower concentration gradient caused slower transport due to decreased diffusion coefficient. The bed gets saturated quickly as the concentration increased. In our study (Table 4) as the dye concentration increased, dye uptake and % removal got increased [44], which might be due to the high driving force observed at higher concentration [15]. The driving force for sorption seemed to be the concentration difference between the dye on the sorbent and dye in the solution. Similar observation was reported by Padmesh et al. [15].

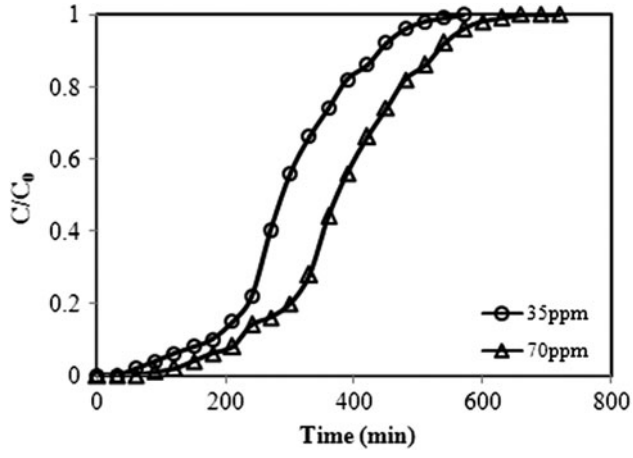

Fig. 8. Breakthrough curves for sorption of redwine dye by *A. filiculoides* at different initial concentrations (15 cm bed height, 2 mL/min, and 30 °C).

3.7. Modeling of column data

3.7.1. Application of BDST model

The BDST model is based on physically measuring the capacity of the bed at different breakthrough values. This model ignores the intraparticle mass transfer resistance and external film resistance such that the adsorbate is adsorbed onto the adsorbent surface directly [15]. The linearity of the plot of the service time against bed height indicated the validity of the BDST Model. The expression is as follows [25]:

$$t = \frac{N_0 Z}{C_0 v} - \frac{1}{K_a C_0} \ln\left(\frac{C_0}{C_b} - 1\right) \quad (15)$$

The service time was chosen as time when the effluent dye concentration reaches 1 mg/L. From the slope of the BDST plot represented in Fig. 9, sorption capacity of the bed per unit volume, N_0 was calculated by assuming the initial dye concentration, C_0, and linear velocity, v as constant during the column operation.

The rate constant, K_a, is calculated from the intercept of the plot and characterizes the rate of solute transfer from the fluid phase to the solid phase [38]. The values of N_0 and K_a were 331.63 mg/g and 0.0173 L/(mg min), respectively. This model helps to scale up the process for other flow rates without further experimental run.

3.7.2. Application of the Thomas model

The column data were fitted to the Thomas model to determine the Thomas rate constant (k_{TH}) and maximum solid phase concentration (q_0) [26,45]. The linearized form of Thomas model can be expressed as follows [46],

$$\frac{C_0}{C} = 1 + \exp\left(\frac{k_{TH}}{F}(Q_0 M - C_0 V_{eff})\right) \quad (16)$$

As flow rate increased, the value of K_{TH} got increased and the q_o got decreased [24]. Also, the bed capacity q_o increased and the Thomas coefficient K_{TH} decreased with increasing dye concentration. It is evident from Table 5 that there was a negligible difference between the experimental data from model predicted values of $q_{0,}$ showing that there was a good fit of Thomas model to the column sorption data.

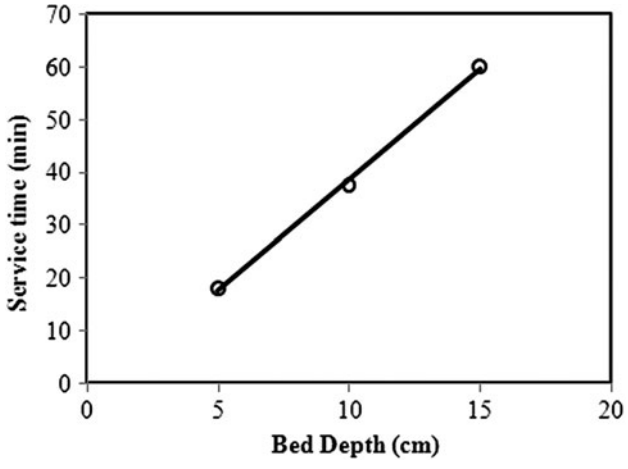

Fig. 9. BDST model plot for sorption of redwine dye by *A. filiculoides*.

3.7.3. Application of the Yoon and Nelson Model

Yoon and Nelson [27] developed a relatively simple model based on the assumption that the rate of decrease in the probability of adsorption for each adsorbate molecule is proportional to the probability of adsorbate adsorption and the probability of adsorbate breakthrough on the adsorbent [25]. The Yoon and Nelson equation regarding the single component system is expressed as [24]:

$$\ln\left(\frac{C}{C_0 - C}\right) = k_{YN} t - \tau k_{YN} \quad (17)$$

The rate constant k_{YN} and τ were determined from the Yoon and Nelson model. From Table 5, it was observed that the time required for 50% adsorbate breakthrough (τ) obtained from the Yoon and Nelson model agreed well with the experimental data at all conditions examined.

3.7.4. Capacity of column

The total or stoichiometric capacity of the packed bed column, if the entire bed comes to equilibrium with the fed, can be shown to be proportional to the area between the curve and a line at C/C_0 at 1.0. The total capacity of the bed is calculated as follows:

$$t_t = \int_0^\infty \left(1 - \frac{C}{C_0}\right) dt \quad (18)$$

where t_t is the time equivalent to the total or stoichiometric capacity.

The usable capacity of the bed up to the break point time t_b is calculated as follows:

Table 5
Thomas and Yoon and Nelson model parameters at different experimental conditions

Bed height (cm)	Flow rate (mL/min)	Dye concentration (mg/L)	$(q_o)_{exp}$ (mg/g)	$(\tau)_{exp}$ (mg/g)	Thomas model			Yoon and Nelson model		
					K_{TH} (L/mg min)	q_o (mg/g)	R^2	k_{YN} (min^{-1})	τ (min)	R^2
5	2	70	2.9	65	1×10^{-3}	2.98	0.956	0.0704	67.77	0.956
5	4	70	2.6	32	1.28×10^{-3}	2.67	0.992	0.0901	32.26	0.992
5	6	70	1.8	11	1.68×10^{-3}	1.7	0.994	0.1189	12.59	0.994
10	2	70	4.09	195	3.71×10^{-4}	4.22	0.976	0.026	197.25	0.991
15	2	35	3.0	375	4.83×10^{-4}	3.32	0.979	0.0169	379.93	0.979
15	2	70	5.4	300	2.56×10^{-4}	5.28	0.994	0.0178	302.7	0.994

$$t_u = \int_0^{t_b} \left(1 - \frac{C}{C_0}\right) dt \quad (19)$$

The ratio t_u/t_t is the fraction of the total bed capacity or length utilized up to the break point. Hence, for a total bed length of H_T, H_B is the length of the bed used up to the break point.

$$H_B = \frac{t_u}{t_t} H_T \quad (20)$$

The length of unused bed H_{UNB} is then the unused fraction times the total length:

$$H_{UNB} = \left(1 - \frac{t_u}{t_t}\right) H_T \quad (21)$$

The results obtained at various experimental conditions are given in Table 6. From Table 6, it is found that almost half of the bed got saturated on reaching the breakthrough point at all experimental conditions.

3.8. Instrumental methods of analysis

3.8.1. Scanning electron microscopy

Morphological characteristics of *A. filiculoides* were evaluated using SEM. The surface texture of *A. filiculoides* biomass without pretreatment, after pretreatment, and after dye binding is shown in Fig. 10(a)–(c). It was observed that the pores present in the surface of *Azolla* before pretreatment (Fig. 10(a)) was found to be less when compared to the *Azolla* after pretreatment with HCl (Fig. 10(b)). This may be due to the shrinkage of *Azolla* surface. From Fig. 10(c), it was observed that the surface became rough because it was covered by dye molecules.

3.8.2. FTIR analysis

FTIR technique is an important tool to identify some characteristic functional groups like carboxyl, hydroxyl, amine, etc. which are capable of adsorbing dye ions. In order to determine the functional groups, *Azolla* was analyzed using FTIR after pretreatment

Table 6
Capacity of column at different column experimental conditions

H_T (cm)	Flow rate (mL/min)	Dye concentration (mg/L)	t_u (min)	t_t (min)	H_B (cm)	H_{UNB} (cm)
5	2	70	25	40.71	3.07	1.93
5	4	70	10	17.9	2.8	2.2
5	6	70	7.86	14.29	2.75	2.25
10	2	70	85.71	160.7	5.3	4.7
15	2	35	180	342.9	7.9	7.1
15	2	70	150	278.6	8.08	6.92

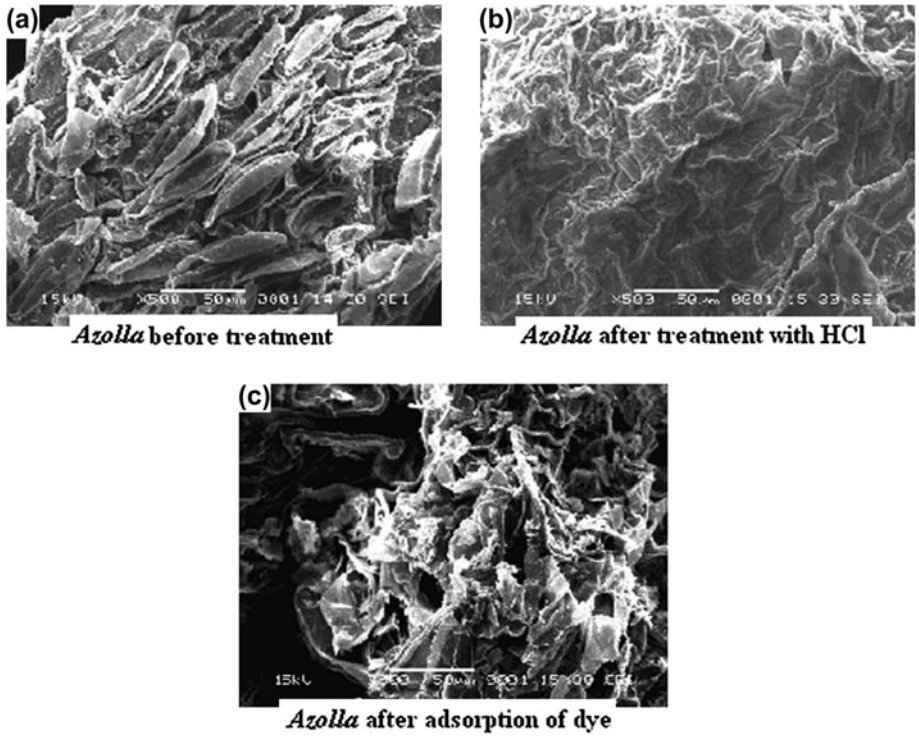

Fig. 10. SEM images of *A. filiculoides* (a) before treatment, (b) after pretreatment with HCl, and (c) after adsorption of dye.

and after dye binding. Fig. 11(a) shows *Azolla* before adsorption in the spectral region of 400–4,000 cm^{-1} and displays a number of absorption peaks, indicating the complex nature of the *Azolla*. The FTIR spectroscopic analysis showed a strong band at 3,800–2,500 cm^{-1}, indicative of –OH in the carboxyl group. The band 2,917.83 cm^{-1} and 2,850.25 cm^{-1} indicate N–H and C–H aliphatic stretch, respectively. The FTIR spectrum showed some characteristic adsorption bands of an amine group N–H bending band at 1,652.11 cm^{-1}. Some absorption bands (P=O stretching at 1,157.08 cm^{-1}; P–OH stretching at 954 cm^{-1}; P–O–C stretching at 1,067.56 cm^{-1} were considered to be indicative of a phosphonate group. Absorbance peaks around 1,157.08 cm^{-1} corresponds to the asymmetric and symmetric stretching of SO_3 bonds in sulfonic acid [47]. Fig. 11(b) shows FTIR analysis of *Azolla* subjected to sorption. Shift in bands and the functional groups peaks reported in Fig. 11(a) were not seen. This confirmed the binding of dye ions to the functional groups carboxyl, sulfonyl, and phosphate.

3.9. COD analysis

COD analysis was performed for dye concentration of 1,000 ppm kept at optimum process conditions before and after sorption and the reduction was observed after treatment with *A. filiculoides*, which indicated that *A. filiculoides* could be a good biosorbent for dye bearing wastewater. The results are tabulated in Table 7.

3.10. Comparison of adsorbent capacities for different biosorbent

The results of this study and the comparison of recent studies are given in Table 8. There are number of studies on the removal of basic and acid dyes by *Azolla*. This study indicated that *A. filiculoides* have potential to be a biosorbent for the removal of reactive dyes from aqueous solution.

4. Conclusion

The following conclusions were drawn from the present study.

- *A. filiculoides* exhibited a maximum uptake at pH 3.0, time 120 min, biomass 1.0 g/L, and temperature 30 °C.
- Biosorption isotherms were modeled with the Langmuir and Freundlich isotherms. The maximum uptake capacity of pretreated *A. filiculoides* for reactive redwine dye biosorption was 86.21 mg/g, according to the Langmuir model.
- The experimental kinetic data showed that the reaction was a pseudo-first-order reaction.

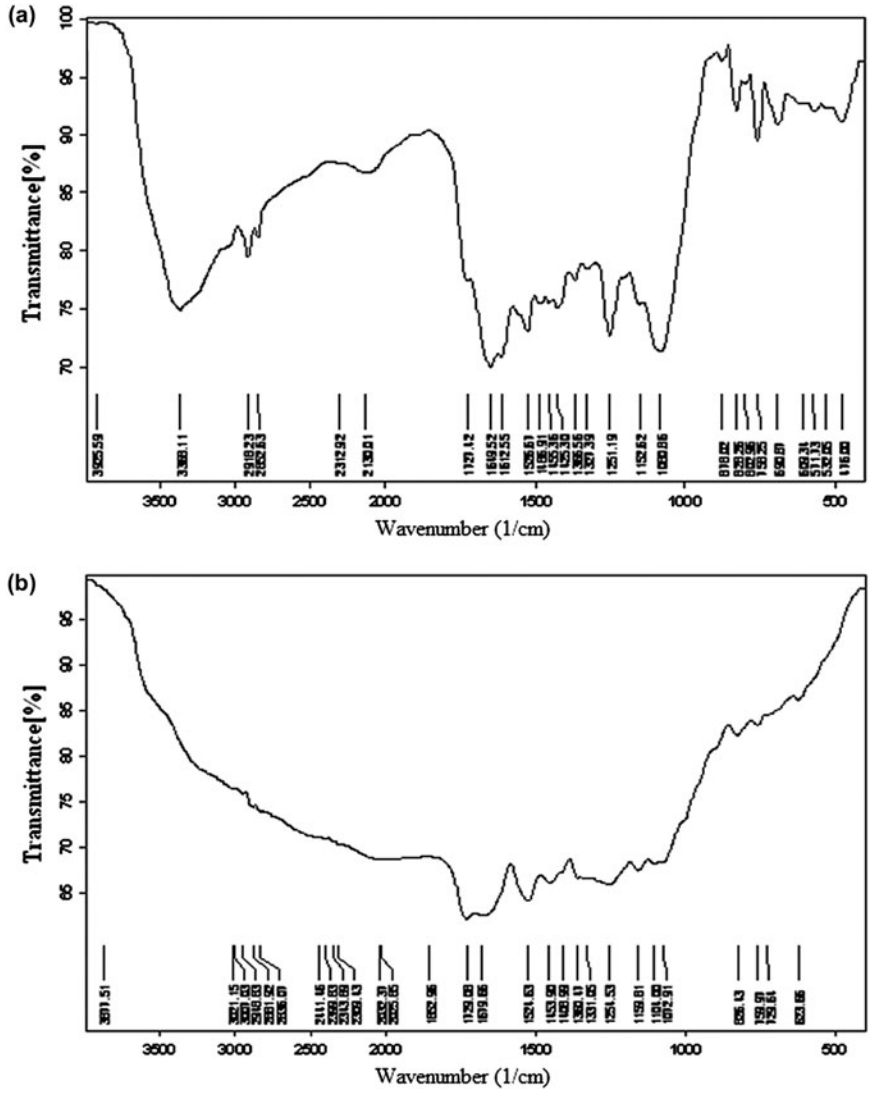

Fig. 11. FTIR analysis of *A. filiculoides* (a) before adsorption and (b) after adsorption.

Table 7
COD analysis before and after treatment

Process parameters	COD values		% Removal
	Before sorption	After sorption	
Optimum process parameters obtained at batch conditions	5,330 mg/L	1,330 mg/L	75.05

- Further the linearity of Boyd plot indicated that film diffusion was the rate-limiting step for the adsorption of redwine dye onto pretreated *A. filiculoides*.
- Thermodynamic parameters confirmed that the sorption process was endothermic and spontaneous in nature.
- Column study concluded that the highest bed height, lowest flow rate, and highest dye concentration showed better uptake on sorption of reactive redwine dye onto pretreated *A. filiculoides*.
- SEM analysis showed the structural changes of biosorbent before and after sorption. The FTIR spectra revealed that the pretreated *A. filiculoides* contained OH group, phosphate, sulfonyl, and carboxyl groups on the surface which might be responsible for the sorption of reactive redwine dye.

Table 8
Comparison of adsorbent capacities for different biosorbents

Adsorbent	Dye	Maximum adsorption capacity (mg/g)	Ref.
Azolla filiculoids	Basic orange	833.33	[16]
	Acid red 88	109.0	[15]
	Acid green 3	133.5	[15]
	Acid orange 7	109.6	[15]
	Reactive redwine	86.21	This work
Lentinus sajor-caju	Reactive red 120	117.8	[30]
Wheat bran	Reactive red 180	39.42	[48]
	Reactive orange 16	34.03	[48]
	Reactive black 5	36.03	[48]
Aspergillus foetidus	Reactive black 5	65.0	[49]
Phanerochaete chrysosporium	Reactive blue 4	132.5	[50]
Waterworks sludge	Reactive orange 16	47	[51]
Barley straw	Reactive black 5	25.4	[52]
Corynebacterium glutamicum	Reactive black 5	419.0	[11]
	Reactive yellow 2	178.5	[53]
Nostoc linckia	reactive red 198	93.5	[54]
Rhizopus arrhizus	Reactive blue 19	90.0	[55]

- COD analysis revealed the fact that *A. filiculoides* was a good biosorbent for the treatment of dye containing wastewater.
- Finally, it could be concluded that *Azolla filiculoides* have a potential to be a biosorbent for the removal of reactive redwine dye from aqueous solutions.

Symbols

λ_{max} — maximum wavelength
q_e — equilibrium dye uptake
C — concentration
C_o — initial dye concentration
C_e — final dye concentration
V — volume of dye solution
M — mass of biomass added
q_{max} — maximum monolayer biosorption capacity
K_L — Langmuir equilibrium constant
K_F — Freundlich constant
n — Freundlich exponent
K_{RP} — Redlich–Peterson model equilibrium constant
a_{RP} — Redlich–Peterson model constant
β — Redlich–Peterson model exponent
K — sips model equilibrium constant
a_S — sips model constant
β_S — sips model exponent
q_t — dye uptake at time "t"
K_1 — pseudo-first-order rate constant
K_2 — pseudo-second-order rate constant
m_{ad} — mass adsorbed
t_b — breakthrough time
t_e — bed exhaustion time
m_{total} — total amount of dye
Q — volumetric flow rate
k_i — intraparticle diffusion parameter
F — fraction of dye mass adsorbed
D_i — effective diffusion coefficient
K_a — sorption equilibrium constant
ΔG° — standard Gibbs free energy
ΔH° — standard enthalpy change
ΔS° — standard entropy change
C_b — breakthrough dye concentration
N_o — sorption capacity of the bed
Z — bed height
v — linear velocity
k_a — rate constant of BDST Model
k_{TH} — Thomas model rate constant
Q_0 — maximum solid-phase concentration of the solute
V_{eff} — volume of dye solution passed into the column
F — volumetric flow rate
k_{YN} — Yoon and Nelson Model rate constant
τ — time required for 50% adsorbate breakthrough
t_t — time equivalent to the total or stoichiometric capacity
t_u — usable capacity of the bed up to the break point time t_b
H_B — length of the bed used up to the break point
H_T — total length of the bed
H_{UNB} — length of unused bed
SEM — scanning electron microscopy
FTIR — Fourier transform infra red spectrophotometer
COD — chemical oxygen demand

References

[1] S.D. Aust, Degradation of environmental pollutants, Microb. Ecol. 20 (1990) 197–209.
[2] T. Robinson, G. Mc Mullan, R. Marchant, P. Nigam, Remediation of dyes in textile effluent: A critical review on current treatment technologies with a proposed alternative, Bioresour. Technol. 77 (2001) 247–255.
[3] J.T. Matheickal, Q. Yu, Biosorption of lead (II) form aqueous solutions by *Phelinus badius*, Miner. Eng. 10 (1997) 87–125.
[4] C. Namasivayam, D. Prabha, M. Kumutha, Removal of direct red and acid brilliant blue by adsorption on to banana pith, Bioresour. Technol. 1 (1998) 77–79.
[5] H. Aydin, G. Baysal, Y. Bulut, Utilization of walnut shells (*Juglans regia*) as an adsorbent for the removal of acid dyes, Desalin. Water Treat. 2 (2009) 139–147.
[6] S. Boutemedjet, O. Hamdaoui, Sorption of malachite green by eucalyptus bark as a non-conventional low-cost biosorbent, Desalin. Water Treat. 8 (2009) 201–210.
[7] A.S. Franca, L.S. Olivera, S.A. Saldanha, P.I.A. Santos, S.S. Salum, Malachite green adsorption by mango (*Mangifera indica* L.) seed husks: Kinetic, equilibrium and thermodynamic studies, Desalin. Water Treat. 19 (2010) 241–248.
[8] E.A. Oliveira, S.F. Montanher, M.C. Rollemberg, Removal of textile dyes by sorption on low-cost sorbents. A case study: Sorption of reactive dyes onto *Luffa Cylindrica*, Desalin. Water. Treat. 25 (2011) 54–64.
[9] Yuzhu Fu and T. Viraraghavan, Column studies for biosorption of dyes from aqueous solutions on immobilized *Aspergillus niger* fungal biomass, Water SA. 29 (2003) 465–472.
[10] A. Ozer, G. Akkaya, M. Turabik, Biosorption of acid blue 290 (AB 290) and acid blue 324 (AB 324) dyes on *Spirogyra rhizopus*, J. Hazard. Mater. 135 (2006) 355–364.
[11] K. Vijayaraghavan, Y.S. Yun, Utilization of fermentation waste (*Corynebacterium glutamicum*) for biosorption of reactive black 5 from aqueous solution, J. Hazard. Mater. 141 (2007) 45–52.
[12] Y. Bayrak, Y. Yesiloglu, U. Gecgel, Adsorption behavior of Cr (VI) on activated hazelnut shell ash and activated bentonite, Microporous Mesoporous Mater. 91 (2006) 107–110.
[13] E. Rubin, P. Rodriguez, R. Herrero, J. Cremades, I. Barbara, M.E.S. de Vicente, Removal of methylene blue from aqueous solutions using a biosorbent *Sargassum muticum*: An invasive macro alga in Europe, J. Chem. Technol. Biotechnol. 80 (2005) 291–298.
[14] B. Volesky, Sorption & biosorption, in: B. Volesky (Ed.), Biosorption of Heavy Metals, Boca Raton, FL: CRC Press, 1990, p. 1–4.
[15] T.V.N. Padmesh, K. Vijayaraghavan, G. Sekaran, M. Velan, Batch and column studies on biosorption of acid dyes on freshwater macroalgae *Azolla filiculoides*, J. Hazard. Mater. 125 (1–3) (2005) 121–129.
[16] Cai-Yun Tan, Min Li, Yu-Man Lin, Lu Xiao-Qiao, Zu-liang Chen, Biosorption of Basic Orange from aqueous solution onto dried *A. filiculoides* biomass: Equilibrium, kinetic and FTIR studies, Desalination 266 (2011) 56–62.
[17] Langmuir, The constitution and fundamental properties of solids and liquids, J. Am. Chem. Soc. 38 (11) (1916) 2221–2295.
[18] H.M.F. Freundlich, Over the adsorption in solution, J. Phys. Chem. 57 (1906) 385–471.
[19] S. Langergren, B.K. Svenska, Zur theorie der sogenannten adsorption geloester stoffe [To the theory of so-called adsorption of dissolved substances], Veternskapsakad Handlingar. 24(4) (1898) 1–39.
[20] Y.S. Ho, G. McKay, Pseudo-second order model for sorption processes, Process Biochem. 34 (1999) 450–465.
[21] Y.S. Ho, G. McKay, The kinetics of sorption of basic dyes from aqueous solutions by sphagnum moss peat, Can. J. Chem. Eng. 76 (1998) 822–826.
[22] APHA, AWWA, WEF, Standard Methods for the Examination of Water and Wastewater, 19th ed., American Public Health Association, Washington, DC, 1995.
[23] B. Volesky, J. Weber, J.M. Park, Continuous-flow metal biosorption in a regenerable Sargassum column, Water Res. 37 (2003) 297–306.
[24] Z. Aksu, F. Gonen, Biosorption of phenol by immobilized activated sludge in a continuous packed bed: Prediction of breakthrough curves, Process Biochem. 39 (2003) 599–613.
[25] R.A. Hutchins, New method simplifies design of activated carbon systems, Chem. Eng. 80 (1973) 133–138.
[26] H.C. Thomas, Heterogeneous ion exchange in a flowing system, J. Am. Chem. Soc. 66 (1944) 1664–1666.
[27] Y.H. Yoon, J.H. Nelson, Application of gas adsorption kinetics. I. A theoretical model for respirator cartridge service time, Am. Ind. Hyg. Assoc. J. 45 (1984) 509–516.
[28] S. Venkata Mohan, J. Karthikeyan, Removal of lignin and tannin aqueous solution by adsorption onto activated charcoal, Environ. Pollut. 1–2 (1997) 183–197.
[29] T.L. Hu, Removal of reactive dyes from aqueous solution by different bacterial genera, Water Sci. Technol. 34 (1996) 89–95.
[30] M. Yakup Arıca and Gulay Bayramoglu, Biosorption of Reactive Red-120 dye from aqueous solution by native and modified fungus biomass preparations of *Lentinus sajor-caju*, J. Hazard. Mater. 149 (2007) 499–507.
[31] F. Banat, S. Al-Asheh, L. Al-Makhedmeh, Evaluation of the use of raw and activated date pits as potential adsorbents for dye containing waters, Process Biochem. 39 (2003) 193–202.
[32] M.S. Chiou, H.Y. Li, Equilibrium and kinetic modeling of adsorption of reactive dye on cross-linked chitosan beads, J. Hazard. Mater. B93 (2002) 233–248.
[33] Y. Nuhoglu, E. Malkoc, A. Gürses, N. Canpolat, The removal of Cu(II) from aqueous solutions by *Ulothrix zonata*, Bioresour. Technol. 85 (2005) 331–333.
[34] V.J.P. Vilar, C.M.S. Botelho, R.A.R. Boaventura, Methylene blue adsorption by algal biomass based materials: Biosorbents characterization and process behaviour, J. Hazard. Mater. 147 (2007) 120–132.
[35] Y.S. Ho, G. McKay, Sorption of dye from aqueous solution by peat, Chem. Eng. J. 70 (1998) 115–124.
[36] K. Marungrueng, P. Pavasant, High performance biosorbent (*Caulerpa lentillifera*) for basic dye removal, Bioresour. Technol. 98 (8) (2007) 1567–1572.
[37] G.E. Boyd, A.W. Adamson, L.S. Myers, The exchange adsorption of ions from aqueous solutions by organic zeolites 2, J. Am. Chem. Soc. 69 (1947) 2836–2848.
[38] D. Mohan, K.P. Singh, Single- and multi-component adsorption of cadmium and zinc using activated carbon derived from bagasse-an agricultural waste, Water Res. 36 (2002) 2304–2318.
[39] R. Aravindhan, J. Raghava Rao, B. Unni Nair, Removal of basic yellow dye from aqueous solution by sorption on green alga *Caulerpa scalpelliformis*, J. Hazard. Mater. 142 (2007) 68–76.
[40] Y.S. Ho, T.H. Chiang, Y.M. Hsueh, Removal of basic dye from aqueous solution using tree fern as a biosorbent, Process Biochem. 40 (1) (2005) 119–124.
[41] N.A. Oladoja, I.A. Ololade, J.A. Idiaghe, E.E. Egbon, Equilibrium isotherm analysis of the sorption of congo red by palm kernel coat, Cent. Eur. J. Chem. 7 (4) (2009) 760–768.
[42] C. Quintelas, B. Fernandes, J. Castro, H. Figueiredo, T. Tavares, Biosorption of Cr (VI) by three different bacterial species supported on granular activated carbon-A comparative study, J. Hazard. Mater. 153 (2008) 799–809.
[43] Z. Zulfadhly, M.D. Mashitah, S. Bhatia, Heavy metals removal in fixed-bed column by the macro fungus *Pycnoporus sanguineus*, Environ. Pollut. 112 (2001) 463–470.
[44] D.C.K. Ko, J.F. Porter, G. McKay, Optimised correlations for the fixed-bed adsorption of metal ions on bone char, Chem. Eng. Sci. 55 (2000) 5819–5829.
[45] R. Senthil Kumar, K. Vijayaraghavan, M. Thilakavathi, P.V.R. Iyer, M. Velan, Seaweeds for the remediation of wastewaters contaminated with zinc (II) ions, J. Hazard. Mater. 136 (3) (2006) 791–799.

[46] G. Yan, T. Viraraghavan, Heavy metal removal in a biosorption column by immobilized *M. rouxii* biomass, Bioresour. Technol. 78 (2001) 243–249.
[47] F. Pagnanelli, M.P. Papini, L. Tora, M. Trifoni, F. Veglio, Biosorption of metal ions on *Anthrobacter* sp.: Biomass characterization and biosorption modeling, Environ. Sci. Technol. 34 (2000) 2773–2778.
[48] Meral Topcu Sulak, H. Cengiz Yatmaz, Removal of textile dyes from aqueous solutions with eco-friendly biosorbent, Desalin. Water. Treat., 37 (2012) 169–177.
[49] Rachna Patel, Sumathi Suresh, Kinetic and equilibrium studies on the biosorption of reactive black 5 dye by *Aspergillus foetidus*, Bioresour. Technol. 99 (2008) 51–58.
[50] Gulay Bayramoglu, Gokce Celik, M. Yakup Arica, Biosorption of reactive blue 4 dye by native and treated fungus *Phanerochaete chrysosporium*: Batch and continuous flow system studies, J. Hazard. Mater. B137 (2006) 1689–1697.
[51] S.W. Won, S.B. Choi, Y.S. Yun, Performance and mechanism in binding of reactive orange 16 to various types of sludge, Biochem. Eng. J. 28 (2006) 208–214.
[52] C. Broto, S.I. Oei, S. Wang, H.M. Ang, Surfactant modified barley straw for removal of acid and reactive dyes from aqueous solution, Bioresour. Technol. 100 (2009) 4292–4295.
[53] S.W. Won, Y.S. Yun, Biosorptive removal of reactive yellow 2 using waste biomass from lysine fermentation process, Dyes Pigm. 76 (2008) 502–507.
[54] Sharma Mona, Anubha Kaushik, C.P. Kaushik, Biosorption of reactive dye by waste biomass of *Nostoc linckia*, Ecol. Eng. 37 (2011) 1589–1594.
[55] T. O'Mahony, E. Guibal, J.M. Tobin, Reactive dye biosorption by *Rhizopus arrhizus* biomass, Enzyme Microb. Technol. 31 (2002) 456–463.